scientific reports

Check for updates

OPEN

Kinetic modelling for concentration and toxicity changes during the oxidation of 4-chlorophenol by UV/H_2O_2

Cristian Ferreiro[1]✉, Josu Sanz[2], Natalia Villota[3], Ana de Luis[4] & José Ignacio Lombraña[1]

This work develops a kinetic model that allow to predict the water toxicity and the main degradation products concentration of aqueous solutions containing 4-chlorophenol oxidised by UV/H_2O_2. The kinetic model was developed grouping degradation products of similar toxicological nature: aromatics (hydroquinone, benzoquinone, 4-chlorocatechol and catechol), aliphatics (succinic, fumaric, maleic and malonic acids) and mineralised compounds (oxalic, acetic and formic acids). The degradation of each group versus time was described as a mathematical function of the rate constant of a second-order reaction involving the hydroxyl radical, the quantum yield of lump, the concentration of the hydroxyl radicals and the intensity of the emitted UV radiation. The photolytic and kinetic parameters characterising each lump were adjusted by experimental assays. The kinetic, mass balance and toxicity equations were solved using the Berkeley Madonna numerical calculation tool. Results showed that 4-chlorophenol would be completely removed during the first hour of the reaction, operating with oxidant molar ratios higher than *R* = 200 at pH 6.0 and UV = 24 W. Under these conditions, a decrease in the rate of total organic carbon (TOC) removal close to 50% from the initial value was observed. The solution colour, attributed to the presence of oxidation products as *p*-benzoquinone and hydroquinone, were oxidised to colourless species, that resulted in a decrease in the toxicity of the solutions (9.95 TU) and the aromaticity lost.

List of symbols

Agitation	Stirring power, rpm
C_0	Initial concentration of 4-chlorophenol, mol L^{-1}
C_{exp}	Concentration of a compound or lump i measured experimentally, mol L^{-1}
C_i	Concentration of each lump i, mol L^{-1}
C_j	Concentration of a given compound present in solution, mol L^{-1}
$C_{HO^\cdot}$	Concentration of hydroxyl radicals, mol L^{-1}
$Colour_0$	Initial colouration was attributed to the 4-chlorophenol in solution, AU
C_{sim}	Concentration of a compound or lump i obtained from the model, mol L^{-1}
C_{TOC}	Concentration of total organic carbon, mol L^{-1}
EC_{50}	Half maximal effective concentration, mol L^{-1}
EC_{50i}	Average half maximal effective concentration, mol L^{-1}
$EC_{50i\ exp}$	Experimentally determined average half maximal effective concentration, mol L^{-1}
F_i	Fraction of UV radiation absorbed by compounds of lump i, dimensionless
I_0	Intensity of the emitted UV radiation, Einstein min^{-1}
IC_{50}	Half maximal inhibitory concentration, mol L^{-1}

[1]Department of Chemical Engineering, Faculty of Science and Technology, University of the Basque Country UPV/EHU, Barrio Sarriena S/N, 48940 Leioa, Spain. [2]Department of Mathematics and Science Didactics, Faculty of Education, Philosophy and Anthropology of Donostia-San Sebastián, University of the Basque Country UPV/EHU, Barrio Sarriena S/N, 48940 Leioa, Spain. [3]Department of Chemical and Environmental Engineering, Faculty of Engineering of Vitoria-Gasteiz, University of the Basque Country UPV/EHU, Nieves Cano, 12, 01006 Vitoria-Gasteiz, Spain. [4]Department of Chemical and Environmental Engineering, Faculty of Engineering in Bilbao, University of the Basque Country UPV/EHU, Plaza Ingeniero Torres Quevedo, 1, 48013 Bilbao, Spain. ✉email: cristian.ferreiro@ehu.eus

k'_1, k'_2, k'_3, k'_4 and k'_5	Pseudo-first-order kinetic constant of each lump, s^{-1}
k_i	Zero-order kinetic constant (oxidation), s^{-1} mol^{-1} L
$\overline{k}_i$	Second order kinetic constant, s^{-1} L mol^{-1}
L	Effective path length of the photoreactor, m
N	Number of experimental values
R	Peroxide/4-chlorophenol molar ratio, dimensionless
t	Time, s
T	Temperature, ℃
Toxicity	Toxicity, TU
V_{reac}	Volume of dissolution, L

Greeks

ε	Molar extinction coefficient, M^{-1} m^{-1}
α	Fraction of all photolytically degraded 4-chlorophenol (group B_1)
σ	Weighted standard deviation
Φ_i	Quantum yield for lump i, mol $Einstein^{-1}$

Subscripts

0	Refers to a time or initial state
A	Refers to the lump formed by 4-chlorophenol
B_1	Refers to the lump formed by hydroquinone, *p*-benzoquinone and other unknown that are more toxic than 4-chlorophenol
B_2	Refers to the lump formed by 4-chlorocatechol, catechol, and other unknown compounds that are less toxic than 4-chlorophenol
C	Refers to the lump formed by formic acid, acetic acid, oxalic acid, and other compounds of similar nature
D	Refers to the lump formed by CO_2 and H_2O
exp	Refers to an experimentally obtained parameter
i	Refers to a certain lump i
j	Refers to the different compounds present in the solution
sim	Refers to a parameter obtained from the kinetic model

Chlorophenols are catalogued as one of the priority pollutants (Clean Water Act and by European Directive 2013/39/EU) according to the United States Environmental Protection Agency (US EPA)[1–3] because they are toxic and potentially carcinogenic compounds[2]. They are considerate one of the most important classes of water contaminants due to they are difficult to remove from the environment[2–5] and they can appear in drinking water when hypochlorite reacts during water disinfection[4]. Thus, they are of great concern.

It have been selected 4-chlorophenol as the representative member of this family of harmful compounds. Levels of 4-chlorophenol have been reported as ranging from 150 µg L^{-1}[6] to 100–200 mg L^{-1}[7,8] in contaminated environments. [10,11].

Advanced oxidation processes (AOPs) could help in the effective removal of these recalcitrant compounds from wastewater[9–11]. However, the cost-inefficiency of these methods limits the practical application of these technologies[12,13]. Moreover, persistent byproducts produced during the oxidation process can be released into the environment[14,15]. Thus, AOPs may be made suitable for industrial applications, if they are adequately integrated with the biological processes by combined treatments. Thus, the complete removal of water pollutants by AOPs could be combined by more environment friendly treatments leading easily biodegradable species. This propose considers that the biological oxidation process could be the last step into a combined oxidation process that results in the complete oxidation of organic load[16,17].

Thus, it is important to develop models that can predict the toxicities of treated solutions for developing integration strategies involving AOPs and biological processes. This tool can be used for the determination of the operating conditions necessary to reduce the toxicity of the system. In this way, it is possible to achieved a water toxicity level that allow the implantation of biological processes where occur the complete degradation of the remaining pollutant load, developing in this way, a cost-effective, integrated wastewater treatment method.

The photochemical degradation of chlorophenols is a well documented process (see Supplementary Table S1). Çatalkaya et al.[18] reported that the UV/H_2O_2 process could effectively reduce the toxicity of the system. This process can also improve biodegradability, decrease the intensity of the colour, and assist in the removal of micropollutants. The use of UV/H_2O_2 is more advantageous than semiconductor photocatalysis due to economic and feasible to implement in an industrial installation. Moreover, the use of a catalyst can lead to some operation problems such as solids management, separation and contamination in the treated water. Other effects such as screening, caused by the presence of suspended solids in industrial wastewaters would lead to a reduction of the efficiency of UV light.

The photolytic decomposition via bond cleavage occurs via a radical mechanism. The hydroxyl radicals (in the presence of oxidants such as H_2O_2) take part in the process as follows[19,20]:

$$H_2O_2 \xrightarrow{h\nu} 2\,HO^{\cdot}. \quad (1)$$

The decomposition of H_2O_2 can be photoinduced by the Haber–Weiss radical mechanism. The propagation steps are as follows:

$$H_2O_2 + HO^{\cdot} \rightarrow H_2O + HO_2^{\cdot}, \quad (2)$$

$$HO_2^{\cdot} + H_2O_2 \rightarrow H_2O + O_2 + HO^{\cdot}. \quad (3)$$

Finally, different termination reactions take place through radical recombination reactions:

$$HO^{\cdot} + HO^{\cdot} \rightarrow H_2O_2, \quad (4)$$

$$HO^{\cdot} + HO_2^{\cdot} \rightarrow H_2O + O_2, \quad (5)$$

$$HO_2^{\cdot} + HO_2^{\cdot} \rightarrow H_2O_2 + O_2. \quad (6)$$

At the same time, dissociation equilibria of the organic compound itself and of the various intermediates formed, such as hydroxyl, hydroperoxide radicals, etc., according to the following:

$$H_2O_2 \rightarrow HO_2^{-} + H^{+}, \quad (7)$$

$$HO_2^{\cdot} \rightarrow H^{+} + O_2^{-}. \quad (8)$$

Like other phenolic compounds, chlorophenols could be degraded to toxic byproducts during the initial stages of the oxidation pathway[3,21], checking that the oxidation intermediates generated could be more toxic than the own parent pollutant (for example quinone like compounds). The formation of these byproducts could be attributed to direct photolysis or the use of low oxidant dosages[22,23]. Then, the efficiency of the oxidant process is generally determined by recording the oxidant dosage per pollutant load containing water. Thus, special attention should be paid to remove completely these toxic intermediates achieving acceptable water quality levels[24]. Consequently, it is necessary operating with excess of oxidant ratios (or an over stoichiometric addition of the oxidant) to avoid the formation of these refractory intermediates, considering that high amounts of oxidant can produce counter-effects leading to increased treatment costs. In this way, the cost-effectiveness of degradation process could be realised by optimising the amount of oxidant to reduce the wastewater toxicity.

Thus, the aim of this work consist of developing a kinetic model based on the oxidant dosage effect allow to predict the toxicity of 4-chlorophenol aqueous solutions oxidised by UV/H_2O_2. Consequently, the water toxicity and the formation of the different reaction intermediates were analysed during the oxidation of 4-chlorophenol. The kinetic model developed grouping three lumps of degradation byproducts as a function of their toxicity degree. The photolytic and kinetic parameters characterising each lump were adjusted in the proposed oxidation assays, obtaining a kinetic model that predict the water toxicity as a function of oxidant dose and the UV exposure time.

Results and discussion

Effect of oxidant dosage on water-quality parameters. Several experiments of 4-chlorophenol oxidation by H_2O_2/UV were carried out at pH 6.0, varying the molar ratios of hydrogen peroxide to 4-chlorophenol between R = 0–400 mol H_2O_2 /mol 4-chlorophenol. The objective was to analyse the effect of the oxidant in the oxidation process, where the parameters considered as water quality indicators were the pollutant concentration (C, mg L^{-1}), total organic carbon (TOC, mg L^{-1}), colour (AU) and loss of aromaticity (AU).

Figure 1a shows that 4-chlorophenol would be completely removed from the system, during the first hour from the start of the reaction, operating with oxidant molar ratios higher than $R = 200$. Under these conditions, a decrease in the rate of TOC removal close to 50% from the initial value was observed (Fig. 1b). These results agrees well with the results (R values in the range of 150–375) reported by Ec et al.[25]. Operating under conditions of lower hydrogen peroxide concentration ($R < 200$), an insufficient amount of hydroxyl radicals is generated, being the photolytic pathway that dominates the radical pathway[26]. As the molar ratio of H_2O_2 to 4-chlorophenol increases, large amounts of the oxidant radicals are generated that assists the effective degradation of 4-chlorophenol. With the dose ratio of H_2O_2 used in this work, as shown in Fig. 1, primary degradation (100%) and mineralisation rate (45% of TOC removal) are achieved, in the same order of variety advanced oxidation techniques, including heterogeneous photocatalytic variants; i.e. with heterojunction[27,28] and hybrid biomaterials[29].

Under conditions of high reactant doses ($R > 200$), hydroxyl radicals were produced in large amounts. The excess H_2O_2 was converted into the hydroperoxyl radical, which exhibits less oxidative power than the hydroxyl radical (Eqs. 2, 7, 8). Additionally, the excess of peroxide was consumed by water and recombination reactions[30]. The solution colour changes during the degradation of 4-chlorophenol (Fig. 1c). Different water colours (purplish-red, reddish-orange, orange, yellow, red-brown, and light yellow) of 4-chlorophenol aqueous solutions oxidised by AOPs have been previously reported[23,31], checking that water colour could be attributed to the presence of degradation by products generated during the oxidation process. The analyses carried out showed that the main by products formed during the oxidation pathways would be *p*-benzoquinone and hydroquinone[32]. The presence of these species would demonstrate that the colour formation is due to the formation of new chromophore groups in benzene rings, causing the generation of quinones and their derivatives[33]. Operating at $R = 200$, colour compounds were oxidized to colourless species, remaining in minor amounts, that resulted in a decrease in the toxicity of the solutions.

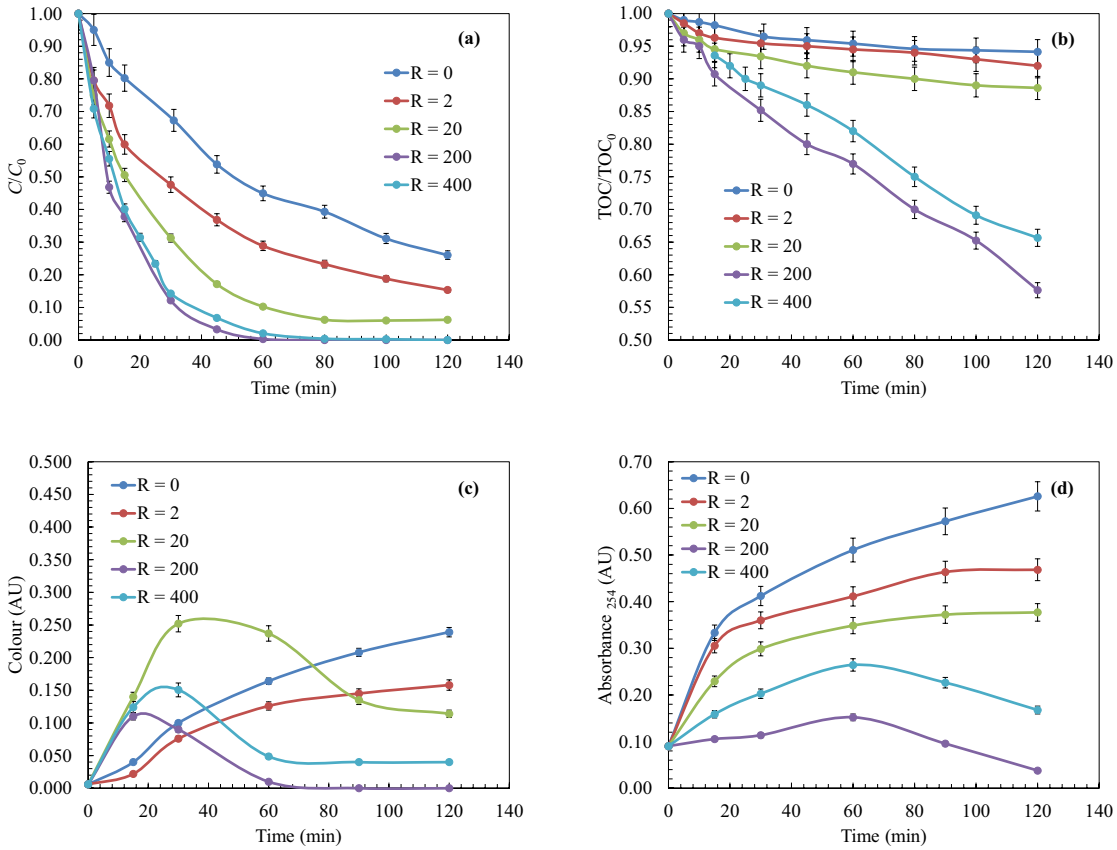

Figure 1. Study of the effect of peroxide dose during the UV/H_2O_2 oxidation of 4-chlorophenol. (**a**) Primary oxidation of 4-chlorophenol; (**b**) Mineralisation; (**c**) Colour induction; (**d**) Aromatic ring rupture. Experimental conditions: $T = 25$ °C; $C_0 = 200$ mg L^{-1}; pH = 6.0; Agitation = 700 rpm; $V_{reac} = 1.7$ L.

The decreased in the loss of aromaticity, analysed at 254 nm, described in Fig. 1d could be attributed to the rupture of the aromatic rings and could indicate the degradation of the aromatic compounds. The loss of aromaticity decreases when $R = 200$, checking that the aromatic rings ruptured and chromophore groups degraded resulting in more favourable oxidation conditions.

Degradation pathway of 4-chlorophenol. Prior to the development of the kinetic model, the pollutant degradation compounds were analysed. Figure 2 shows the degradation of 4-chlorophenol, as well as the formation of their main oxidation intermediates. Results show that the oxidation of 4-chlorophenol leads to the formation of intermediate species of aromatic nature such as 4-chlorocatechol, catechol, hydroquinone and *p*-benzoquinone, as well as the formation of aliphatic species, such as maleic, fumaric, formic and acetic acids. The results obtained allow to verify that the action of UV light is capable of degrading the 4-chlorophenol rings to dihydroxylated rings (Fig. 2a). However, UV light did not prove effectiveness during the degradation of dihydroxylated intermediates to quinone-like compounds and carboxylic acids (Fig. 2b).

Thus, with the aim of degrade 4-chlorophenol until achieve higher oxidation levels, it is necessary to combine UV light with the action of an oxidant (hydrogen peroxide). Figure 1c,e show that the main degradation pathway of 4-chlorophenol evolves towards the formation of chlorosubstituted intermediates (chlorocatechol). On the other hand, once the aromatic intermediates have been degraded until carboxylic acids, it can be checked that using oxidant ratios of $R = 200$, 4-chlorophenol was completely degraded until formic acid.

The analysis performed suggests two possible reaction pathways[34]. In the first, the hydroxyl radicals attacks the aromatic rings in the *ortho*-substituted position, and displaces hydrogen, which promotes the formation of 4-chlorocatechol. In the second, the attack of hydroxyl radicals can occur in the *para*-substituted position, which cause the displacement and substitution of the chloride ion, causing the formation of hydroquinone, which is oxidised to benzoquinone (see Fig. 3).

Kinetic modelling of the reaction intermediates pathway. Determination of the reaction kinetics of such complex oxidation processes can be simplified using a lumped model where all the species exhibiting similar characteristics are grouped. Thus, each group was regarded as a unique compound[35]. The contributions of different oxidation intermediates towards the total toxicity of the system depend on their individual toxicities. Then, all the oxidation intermediates do not contribute equally to the total toxicity of the system. The oxidation by products are grouped into five main groups based on their toxicity. The lumped model was constructed fol-

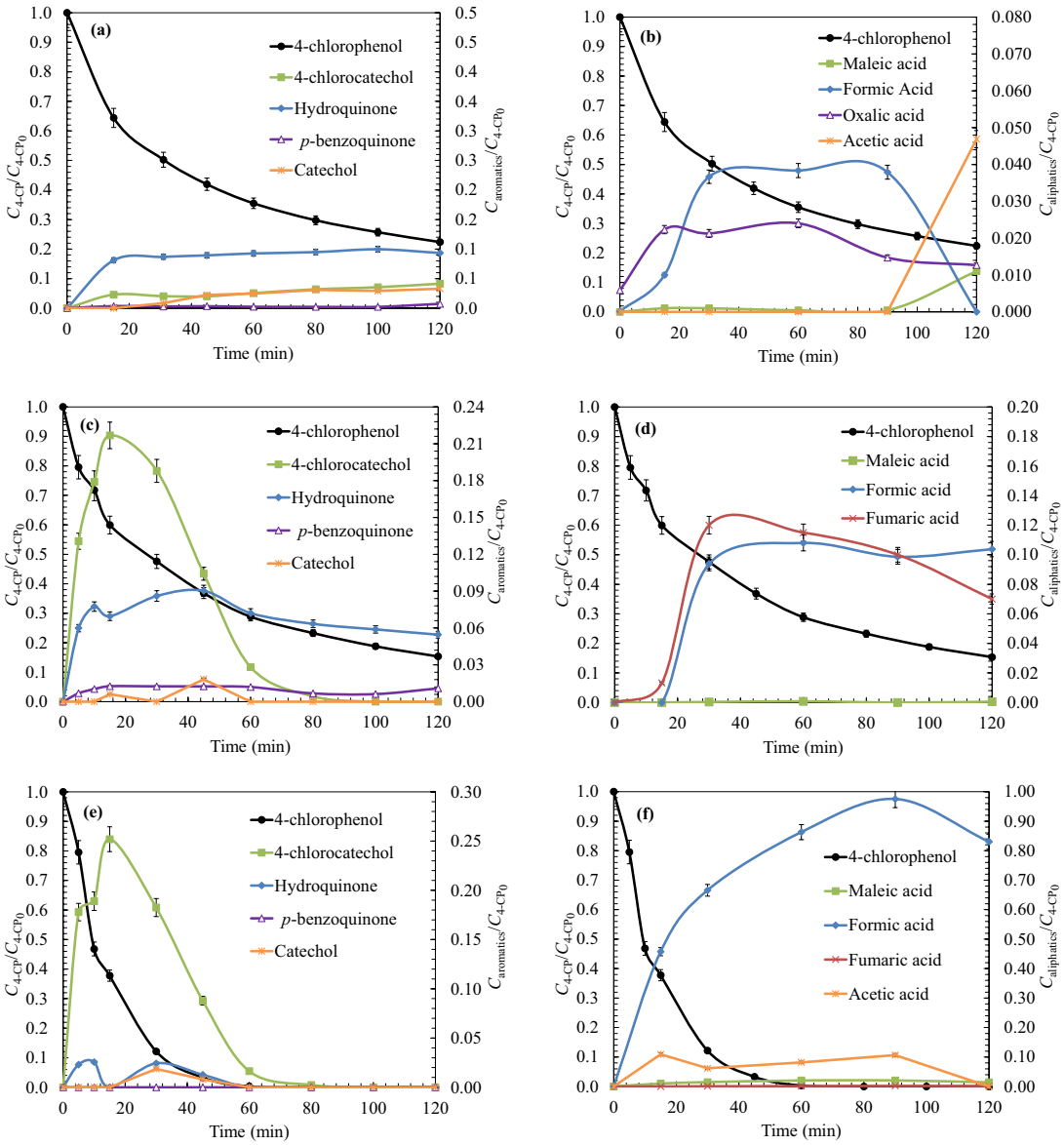

Figure 2. Analysis of the main degradation intermediates (left: aromatic compounds; right: aliphatic oxidation products) produced during the oxidation of 4-chlorophenol (UV/H_2O_2 process) under different peroxide doses: (**a**)/(**b**) $R = 0$; (**c**)/(**d**) $R = 2$; (**e**)/(**f**) $R = 200$. Experimental conditions: $T = 25$ °C; $C_0 = 200$ mg L^{-1}; pH = 6.0; Agitation = 700 rpm; $V_{reac} = 1.7$ L.

lowing previously reported protocols[24]. The mechanisms proposed by Kusic et al.[36] and Gomez et al.[3] have been presented in Fig. 4.

A common photolytic process forms the basis of the first stage of the oxidation process (4-chlorophenol oxidation; assigned as A). Direct photolysis promotes hydroxylation and dechlorination reactions. The highly toxic *p*-benzoquinone ($EC_{50} = 0.035$ mg L^{-1}) and/or hydroquinone ($EC_{50} = 0.088$ mg L^{-1}) intermediates[37], and comparatively less toxic 1,2,4-trihydroxybenzene ($EC_{50} = 1.03$ mg L^{-1}) and/or resorcinol ($EC_{50} = 9.02$ mg L^{-1}) were produced in small amounts[35].

The hydroxyl radicals turned the oxidation process via another oxidation pathway that results in the formation of other substances like hydroquinone. Chlorinated compounds and *p*-benzoquinone were also formed during the process. Aromatic compounds of varying toxicities were formed in the first step of the oxidation process. Group B_1 consists of *p*-benzoquinone and hydroquinone. These compounds are believed to contribute the most maximum towards the global toxicity of treated wastewater as these compounds are abundant[24]. Several researchers have reported that condensation products were formed within minutes (from the start of the reaction) in the absence of oxidants (or under conditions of oxidant deficiency). The majority of the by products formed, were two-ring aromatic chlorinated compounds such as chlorinated hydroxylated biphenyls, dichlorodiphenyl ethers, and dichlorodibenzodioxins. These chlorinated compounds significantly raise the toxicity of the system[22].

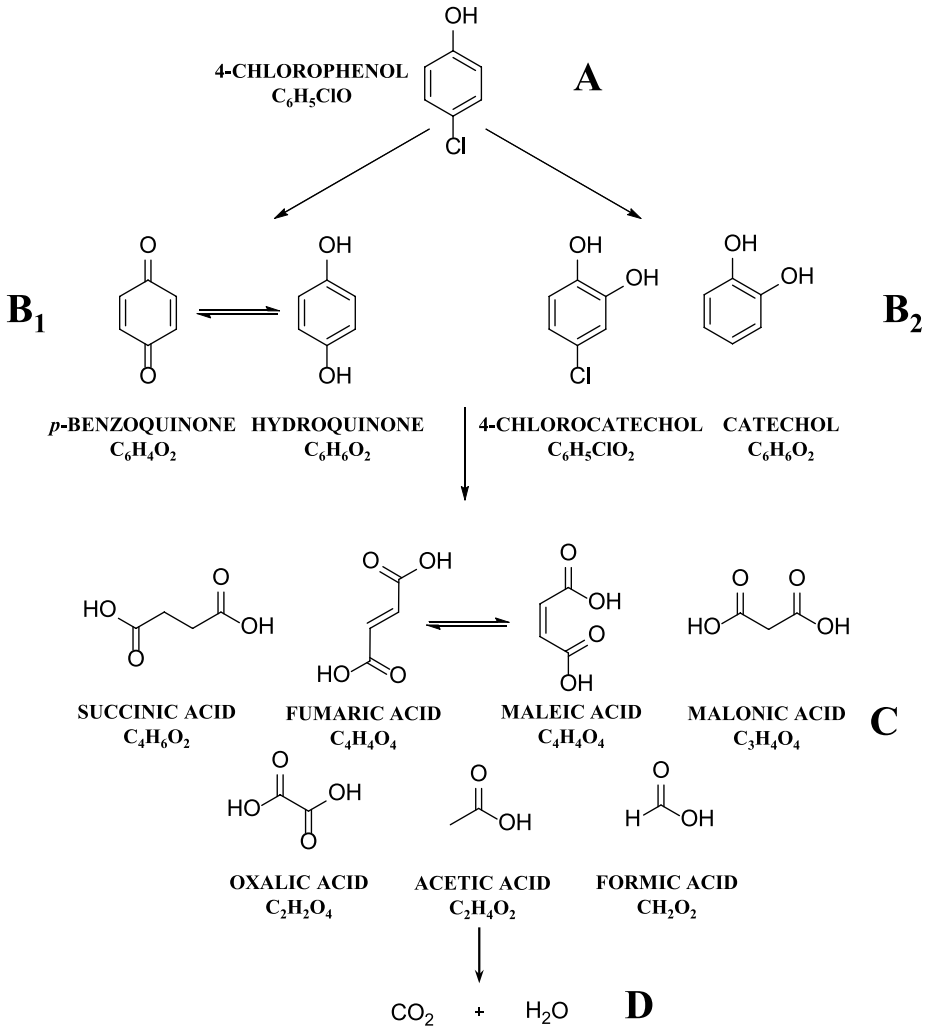

Figure 3. Proposed oxidation pathway for the oxidation of 4-chlorophenol via UV/H_2O_2 process.

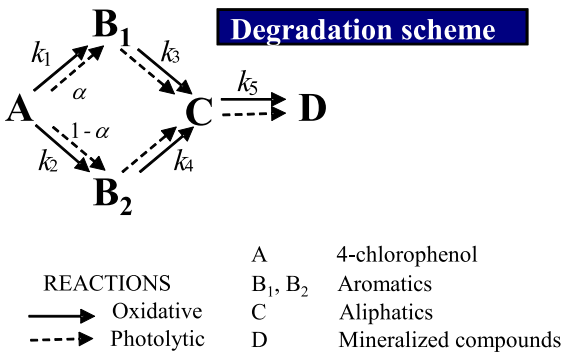

Figure 4. Proposed parallel reaction model for the oxidation of 4-chlorophenol using the UV/H_2O_2 technology.

In this case, water appeared yellow–brown, indicating the presence of these chromophoric toxic compounds with high molecular weight[32].

The aromatic 4-chlorocatechol and catechol compounds formed as by products via the radical pathway are members of the B_2 group. These compounds are less toxic than the parent compounds. In the next step of oxidation, aromatic compounds were converted to unsaturated acids (fumaric acid and maleic acid) that are subsequently converted to saturated carboxylic acids (formic acid and acetic acid). Among these, formic acid,

acetic acid, fumaric acid, and maleic acid are members of group C. The constituents of this group were less toxic than the constituents of the previously described groups. Further oxidation results in CO_2 mineralisation and formation of water (group D)[36,38].

The change in the concentrations of the species of each group over time and the variation in toxicity over time can be determined using a kinetic model. The model was proposed by studying the reaction mechanism presented in Fig. 4. Various factors were considered for developing the kinetic model:

- Three groups (lumps) of oxidation intermediates (B_1, B_2, and C) were defined. Group B_1 primarily consisted of hydroquinone, *p*-benzoquinone, and some unknown compounds (of similar structure) that exhibited high toxicity[24]. Groups B_2 and C consisted of compounds that exhibited lower toxicity levels. The toxicity levels and the constituents were experimentally determined. Group B_2 consisted of 4-chlorocatechol and catechol and group C consisted of various carboxylic acids (acetic acid, oxalic acid, formic acid, succinic acid, malonic acid, maleic acid, and fumaric acid).
- The degradation of 4-chlorophenol proceeds via a two ways parallel reaction mechanism. The mechanism has been previously reported by Azevedo et al.[39] (Fig. 4). B_1 and B_2 are the reference lumps of each route.
- The degradation of each group proceeds via the photolytic (zero-order kinetic (k_i)) and radical (pseudo-first-order kinetic (k'_i)) pathways.
- The average toxicity (EC_{50}), photolytic parameters, and kinetics constants have been determined for each lump. The experimentally obtained values of toxicity and concentration were fitted using the appropriate analysis model.

The degradation of each group versus time is described by Eq. (9), which considers the contributions of the direct photolysis and hydroxyl-radical attack processes[3,35,40]. The relation can be expressed as follows:

$$-\frac{dC_i}{dt} = I_0 \times \Phi_i \times F_i \times \left(1 - \exp\left(-2.303 \times L \times \sum\left(\varepsilon_j \times C_j\right)\right)\right) + \overline{k}_i \times C_i \times C_{HO^{\cdot}}, \tag{9}$$

where $\overline{k}_i$ is the rate constant of a second-order reaction involving the hydroxyl radical in group i, Φ_i denotes the quantum yield of lump i, $C_{HO^{\cdot}}$ denotes the concentration of the hydroxyl radicals, and I_0 represents the intensity of the emitted UV radiation. F_i (incident radiation) denotes the radiation absorbed partially by each group. This can be expressed by Eq. (10) as follows:

$$F_i = \frac{\sum\left(\varepsilon_j \times C_j\right)_i}{\sum \varepsilon_j \times C_j}. \tag{10}$$

Equation (9) could be simplified if it was assumed that the reaction between hydroxyl radicals and 4-chlorophenol is a pseudo-first-order reaction (k'_i)[19,41]. Under this condition, mass balance equations can be formulated for 4-chlorophenol (group A). The other four degradation products are grouped (groups B_1, B_2, C, and D) based on the total organic carbon (TOC) values. The simplified equations can be expressed as follows:

$$\frac{dC_A}{dt} = -I_A \times \Phi_A \times F_A - k'_1 \times C_A - k'_2 \times C_A, \tag{11}$$

$$-\frac{dC_{B_1}}{dt} = \alpha \times I_A \times \Phi_A \times F_A - I_{B_1} \times \Phi_{B_1} \times F_{B_1} + k'_1 \times C_A - k'_3 \times C_{B_1}, \tag{12}$$

$$-\frac{dC_{B_2}}{dt} = (1-\alpha) \times I_A \times \Phi_A \times F_A - I_{B_2} \times \Phi_{B_2} \times F_{B_2} + k'_2 \times C_A - k'_4 \times C_{B_2}, \tag{13}$$

$$-\frac{dC_C}{dt} = I_{B_1} \times \Phi_{B_1} \times F_{B_1} + I_{B_2} \times \Phi_{B_2} \times F_{B_2} - I_C \times \Phi_C \times F_C + k'_3 \times C_{B_1} + k'_4 \times C_{B_2} - k'_5 \times C_C, \tag{14}$$

$$-\frac{dC_D}{dt} = I_C \times \Phi_C \times F_C + k'_5 \times C_C, \tag{15}$$

$$-\frac{dC_{TOC}}{dt} = k'_1 \times C_A + k'_2 \times C_{B_1} + k'_3 \times C_{B_2} + k'_4 \times C_C + k'_5 \times C_D, \tag{16}$$

where α denotes the photolytically degraded fraction of 4-chlorophenol to group B_1 and C_i denotes the concentration of each lump i. The change in toxicity over time can be predicted by studying the toxicities exhibited by each lump. The concentration at any given time and the average toxicity of each group was predicted by preliminary calculations and validated from results reported in the literature (Table 1). Group D was excluded from the calculations as mineralised CO_2 and water were present in the system. It did not contributed to the overall toxicity of the system. Toxicity was determined by Eq. (17), which was derived from Eq. (19). The equation derived to determine the toxicity of the system takes into account the fraction of unknown compounds belonging to group B_1. The following equation was proposed to determine the toxicity of the system based on the above assumptions[24]:

Substance group	Compound	EC_{50} (mg L^{-1})		ε (M^{-1} cm^{-1})		Φ (mol $Einstein^{-1}$)	
		Individual	Lump	Individual	Lump	Individual	Lump
A	4-chlorophenol	5.654	5.654	510.0	510.0	0.017	0.017
B_1	Hydroquinone	0.088	0.0615	307.2	2044.9	0.047	0.025
	p-benzoquinone	0.035		13,612.0		0.025	
B_2	4-chlorocatechol	5.932	6.892	381.3		0.057	0.0024
	Catechol	7.853		504.1		0.0001	
C	Maleic acid	3.852	63.154	769.9	1172.0	0.048	0.0351
	Fumaric acid	15.79		894.0		0.063	
	Malonic acid	12.28		697.0		0.27	
	Oxalic acid	817.2		630.9		0.15	
	Acetic acid	273.2		3159.2		0.028	
	Formic acid	235.6		504.1		0.006	
	Succinic acid	102.0		6300.0		0.0032	

Table 1. Toxicity and photolytic properties of individual and grouped substances produced during the oxidation of 4-chlorophenol (UV/H_2O_2 oxidation mechanism)[36,38,42–44].

Group	ε (M^{-1} cm^{-1})	Φ (mol $Einstein^{-1}$)	EC_{50} (mg L^{-1})
A	409	0.022	4.068
B_1	480	0.015	0.075
B_2	325	0.007	6.240
C	1485	0.005	73.300
D	–	–	–

Table 2. Photolytic and toxicity properties determined using the proposed toxicity—kinetic model. Experimental conditions: $T = 25$ °C; $C_0 = 200$ mg L^{-1}; pH = 6.0; Agitation = 700 rpm; $V_{reac} = 1.7$ L.

$$-\frac{\mathrm{d}Toxicity}{\mathrm{d}t} = k_1' \times \frac{C_A}{EC_{50_A}} + k_2' \times \left(\frac{C_{B1}}{EC_{50_{B1}}} + \frac{C_{B1unk}}{EC_{50_{B1}}}\right) + k_3' \times \frac{C_{B2}}{EC_{50_{B2}}} + k_4' \times \frac{C_C}{EC_{50_C}} \quad (17)$$

Validation of the kinetic model. The model proposed was based on the lumped mechanism described by Kusic et al.[36] and Li et al.[45]. The kinetic, mass balance, and toxicity equations were solved using the Berkeley Madonna numerical calculation tool (Eqs. 10–17). The change in the concentration of each lump over time was determined using this method.

The simultaneous fitting of experimental and simulated data helped to determine the simulated photolytic, kinetic, and toxicity values of each lump. The determination of these values and the EC_{50} values of the compounds can potentially help to predict the toxicity of wastewater during the UV/H_2O_2 treatment process, carried out under different operational conditions. The adjustment minimises the sum of squared residuals. The goodness of fit was determined by calculating the weighted standard deviation, σ, given by Eq. (18) as follows[30]:

$$\sigma = \sqrt{\frac{\sum_{i=1}^{N}\left(\frac{C_{exp}-C_{sim}}{C_{exp}}\right)^2}{N-1}}, \quad (18)$$

where N was the number of experimental values and C_{exp} and C_{sim} denote the concentration (of the compound or lump (i) determined experimentally and the concentration determined using the model, respectively. The data obtained from the direct photolysis experiments ($R = 0$) were used to determine the values of the photolytic parameters (quantum yield and extinction coefficient). The process of direct photolysis only affects the rate of disappearance of each lump. The photolytic contribution can be determined from the Lambert–Beer law. The initial values of the quantum yield (Φ) and extinction coefficient (ε) were presented in Table 1. After determining the photolytic parameters (Table 2), the experimental data were modelled in the presence of H_2O_2 to determine the values of the pseudo-first-order rate constants (k'_1, k'_2, k'_3, k'_4, and k'_5). The constants can be estimated by studying the reactions between the hydroxyl radicals and the lumps (except D; Eqs. 11–14). For the direct photolysis process ($R = 0$), the zero-order kinetic constants (k_i) and the condition of total mass balance (Eq. 16) were considered for determining the experimental and theoretical concentrations of each group. The simulated constants were presented in Table 2. Following this, it was determined if the $EC_{50i\ sim}$ values of each group (obtained by fitting the simulated toxicity data) agreed well with the experimentally obtained $EC_{50i\ exp}$ values of each lump. The initial EC_{50i} values were determined using the EC_{50} values of the individual species

Parameter	UV alone process			
k_1 (s^{-1} mol L^{-1})	2.12×10^{-5}			
k_2 (s^{-1} mol L^{-1})	0.99×10^{-5}			
k_3 (s^{-1} mol L^{-1})	1.30×10^{-5}			
k_4 (s^{-1} mol L^{-1})	4.64×10^{-5}			
k_5 (s^{-1} mol L^{-1})	1.48×10^{-5}			
α	0.37			
σ	0.054			
	UV/H_2O_2 process			
	$R=2$	$R=20$	$R=200$	$R=400$
k'_1 (s^{-1})	2.46×10^{-5}	1.51×10^{-4}	6.87×10^{-4}	2.05×10^{-4}
k'_2 (s^{-1})	1.07×10^{-5}	1.16×10^{-3}	1.25×10^{-3}	1.19×10^{-3}
k'_3 (s^{-1})	1.54×10^{-5}	5.83×10^{-5}	1.23×10^{-4}	8.56×10^{-5}
k'_4 (s^{-1})	4.96×10^{-5}	1.65×10^{-4}	1.14×10^{-3}	4.44×10^{-4}
k'_5 (s^{-1})	1.67×10^{-5}	4.50×10^{-5}	9.10×10^{-5}	6.82×10^{-5}
α	0.35	0.21	0.16	0.19
σ	0.057	0.043	0.052	0.049

Table 3. Kinetic parameters predicted using the proposed toxicity—kinetic model at different H_2O_2/4-chlorophenol ratios. Experimental conditions: $T=25$ °C; $C_0=200$ mg L^{-1}; pH = 6.0; Agitation = 700 rpm; $V_{reac}=1.7$ L.

reported in the literature[36,38,42–44]. The values obtained from literature reports have been presented in Table 1. It is worth mentioning that the toxicities exhibited by the substances (belonging to the same group) were similar (EC_{50} values of the same order of magnitude). This was the primary criterion of lumped modelling.

High quantum yields were recorded for groups A and B_1 (0.022 and 0.015 mol Einstein^{-1}, respectively; Table 2). The data revealed that 4-chlorophenol could be easily degraded by the process of direct photolysis[41]. The branch mechanism is favoured when the photolytic pathway is the predominant mechanistic pathway. It was observed that a satisfactory adjustment between the simulated and experimental results could be achieved ($\sigma \cong 0.05$) if a quantum yield value (for the reaction involving the photolysis of 4-chlorophenol), that is close to that reported by Pera-Titus et al.[46] is used for the calculations. The quantum yield recorded for group C (Φ = 0.005 mol Einstein^{-1}), which consists of aliphatic compounds, agreed well with the quantum yield reported by Kralik et al. for the same group[40].

As mentioned before, the theoretical toxicity of each group was represented as a function of the EC_{50} values of the identified species. The Microtox toxicity bioassay was used to determine the values presented in Table 2. The experimentally determined values were compared with the values presented in the literature (Table 1).

Table 3 presents the values of the kinetic constants determined using the proposed kinetic model. The value of α (the coefficient that correlates the production of substances (by photolytically degrading A) belonging to group B_1 to the compounds belonging to group B_2) was found to be 0.37. It must be remembered that the models comprised of compounds that exhibited similar toxicological properties. Group B_1 comprised of all unknown aromatic compounds.

The results reveal that in the absence of oxidants, the highly toxic compounds, such as double-ringed chlorinated compounds (except *p*-benzoquinone and hydroquinone), were produced[47]. This was because, during the photolytic oxidation process, the formation of hydroquinone or *p*-benzoquinone was favoured over the formation of 4-chlorocatechol[36]. The experimental results presented in Table 3 validate this result. The coefficient α, determined using the simulation method, helps in understanding the nature of the unidentified products. The value of α (0.37) indicates that under these conditions, oxidation products that were more toxic than the parent pollutants were formed. Among all the identified compounds, hydroquinone was found to be present in the highest amount[48]. On the other hand, the value of this fraction decreased to 0.16 (at $R=200$) when experiments were carried out in the presence of H_2O_2.

The values of the kinetic constants indicate that k_1 (2.12×10^{-5} s^{-1} mol L^{-1}) was higher than k_2 (0.99×10^{-5} s^{-1} mol L^{-1}) (under conditions of all oxidant dosages). The differences between k'_1 and k'_2 increased as the peroxide concentration increases. At conditions of $R=200$, this difference increaseed by two orders of magnitude ($k'_2=1.25\times10^{-3}$ s^{-1} versus $k'_3=1.23\times10^{-4}$ s^{-1}; Table 3). These results reveal that the radical pathway promotes the formation of the constituents of group B_2 (over the constituents of group B_1). This result has been previously reported by other groups[35,40,49]. It has been hypothesised that when the oxidation reaction occurs in the presence of hydroxyl radicals, the hydroxylation reaction was favoured over the chlorination reaction. This was because the *para*-position of chlorophenol is highly susceptible to attack during the direct photolysis reactions. The photoreactivity of the chlorine atom is higher than that of the hydroxyl group. In the presence of peroxides, chlorophenols react rapidly under conditions of UV radiation[41].

Under maximum dosage conditions, a large amount of 4-chlorocatechol was degraded and less amounts of *p*-benzoquinone (or hydroquinone) was produced. Similar results were obtained when the k'_1 values at different H_2O_2 dosages were compared with each other. The value of k'_1 increased as the value of R increase (from

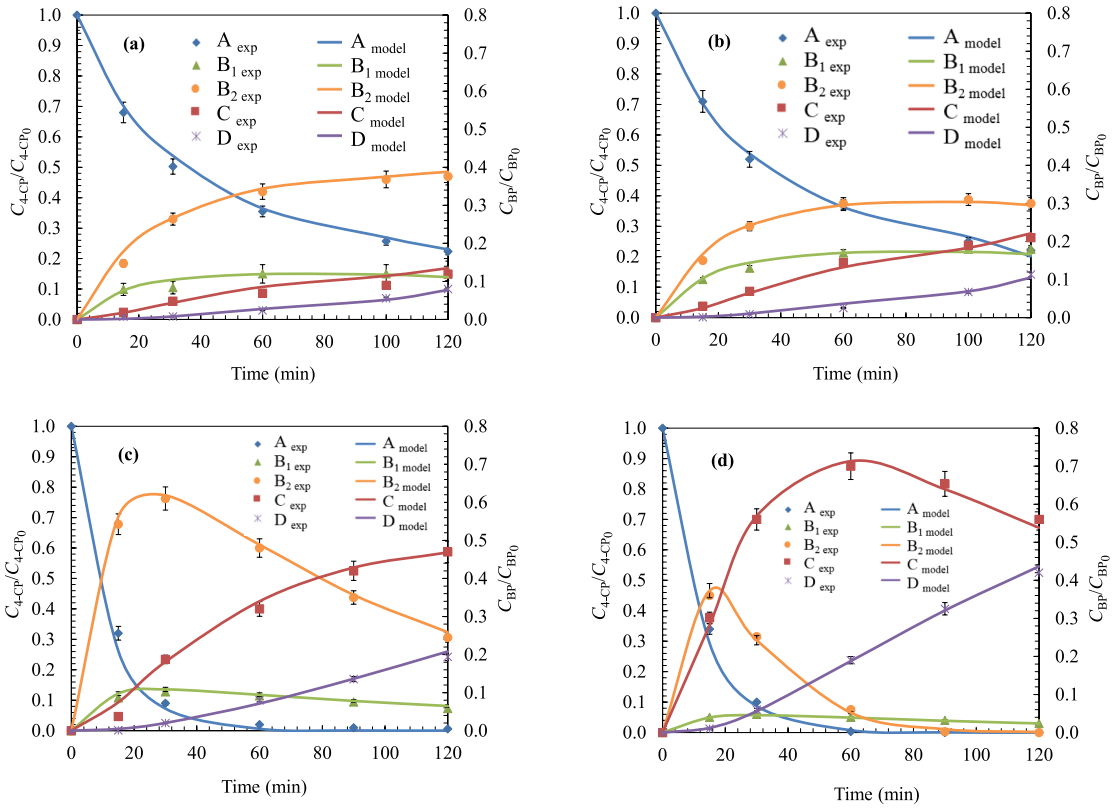

Figure 5. Evolution of the dimensionless concentration of each lump during the oxidation of 4-chlorophenol. Data fitted to the kinetic model at different doses of H_2O_2: (**a**) $R=0$; (**b**) $R=2$; (**c**) $R=20$; (**d**) $R=200$. Experimental conditions: $T=25$ °C; $C_0=200$ mg L^{-1}; pH = 6.0; Agitation = 700 rpm; $V_{reac}=1.7$ L.

$R=2$ (2.46×10^{-5} s^{-1}) to $R=20$ (1.51×10^{-4} s^{-1})). A slight drop in value was observed when R was in the range of 200–400 ($R=200$ (6.87×10^{-4} s^{-1}); $R=400$ (2.05×10^{-4} s^{-1})). The amount of hydroxyl radicals present in the media ($R>200$) hindered the production of the compounds constituting group B_1. Simultaneously, the formation of the compounds constituting group B_2 was promoted (Fig. 5. The values of k'_1 and k'_2 indicated the efficiency with which 4-chlorophenol was degraded.

The results revealed that the values of the kinetic constants (k'_1 and k'_2) increase till $R=200$ and become constant thereafter. It was observed that the amounts of degraded compounds did not increase with the increase in the amount of oxidant under conditions of constant radical concentration. A lower concentration of the generated hydroxyl radicals under steady-state conditions did not promote the efficiency of the reaction. The oxidant dosage under these conditions was known as the critical dose. When the critical R-value was reached, an increase in the peroxide dosage can potentially hinder the oxidation reaction, as the excess hydroxyl radicals can potentially react with H_2O_2 (scavenger reactions)[1,18]. Similar observations were made when the change in the concentration of 4-chlorophenol with time was experimentally studied under conditions of $R=20$ (Fig. 5c) and 200 (Fig. 5d).

The critical dose under which the process of mineralisation or complete degradation was not promoted, was approximately 200 ($R=200$). Although the reaction kinetics (direct oxidation of 4-chlorophenol) was not improved when the dosage was increased above 20, the analysis of the experimental results revealed that rate of mineralisation increased with the increase in the oxidant dosage. The concentration of the different oxidation products decreased at a higher rate under the experimental conditions. This was validated by the k'_4 and k'_5 values determined by the simulation experiments (Table 3). The values of the constants k'_4 and k'_5 indicated that when the dose of H_2O_2 was increased, the rate of mineralisation increased. This was reflected by the increase in the amounts of low molecular weight compounds (such as fumaric acid). The values of the constants k'_1 and k'_2, directly related to the primary degradation of *p*-chlorophenol, remained constant ($R\geq20$). However, the values of the other constants increased under similar conditions.

Aromatic compounds (constituents of groups B_1 and B_2) were the reactants in the second step of the oxidation reaction. The rate of the final step (group D; CO_2 and H_2O) rapidly increased at $R=200$. The critical R for mineralisation was reached at dosages >200, though the maximum amounts of the compounds that belong to group B_2 were formed within the first 20 min of the reaction. On the other hand, the amounts of compounds (carboxylic acids and low molecular weight compounds) constituting group C increased (Fig. 5d) till the first 60 min. Following this, the amounts of the compounds decreased as hydroxyl radicals (generated from H_2O_2) increased. These radicals could effectively react with these compounds to produce increased amounts of CO_2 and H_2O (group D).

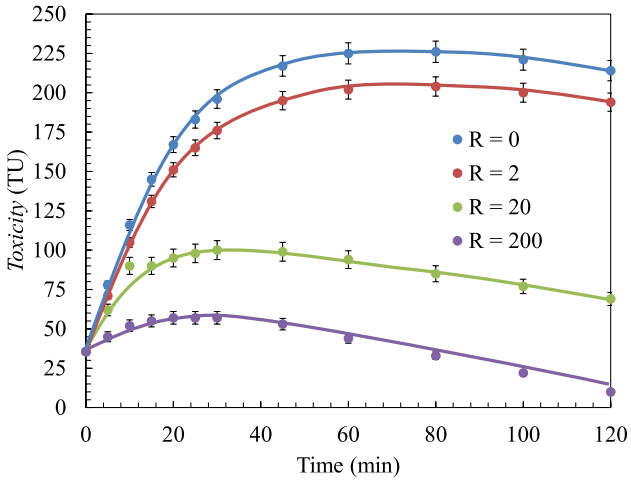

Figure 6. Prediction of the toxicity of the mixture during the oxidation of 4-chlorophenol (UV/H_2O_2 process) varying H_2O_2 dose.

Figure 6 showed the change in toxicity over time, determined using the kinetic model, at four different doses of peroxide during the process of photolysis. Good fitting results were obtained and the mean standard deviation was approximately 0.057 ($\sigma \cong 0.057$). The toxicity was found to increase during the first 20 min of the reaction. Compounds belonging to group B_1 (such as hydroquinone and *p*-benzoquinone) that were more toxic than 4-chlorophenol were produced under these conditions. An increase in the dose of H_2O_2 resulted in a decrease in the amounts of the compounds. The degradation compounds belonging to groups B_1 and B_2 were removed from the system under these conditions and by products (such as formic acid or fumaric acid) belonging to group C (less toxic compounds) were formed.

This increase in toxicity was also reported by Muñoz et al.[22] and Karci et al.[23] that they concluded that in the absence of oxidant or under conditions of inadequate oxidant dose, toxic substances (such as hydroquinone and *p*-benzoquinone) and condensation by products were formed. According to Ronco et al.[50], a toxicity value of less than 1 TU indicated that the effluent was non-toxic or exhibited low toxicity. The values in the range of 1–10 TU correspond to slightly toxic effluents. When the value > 11 TU, the effluent was considered to be highly toxic. At $R = 200$, a value of 9.95 TU was recorded for the wastewater under study. This sample could be used for biodegradation. The degradation pathway led to the formation of the compounds constituting group B_1 under conditions of inadequate doses of oxidants. Under these conditions, the original wastewater sample was found to be more toxic and the chemical degradation pathway could not be complemented by a biological process.

Methods

Reagents. 4-Chlorophenol (ClC_6H_4OH, Sigma-Aldrich, ≥ 99%), hydrogen peroxide (H_2O_2, Labkem, 30%, (v/v)), hydrochloric acid (HCl, Sigma-Aldrich, 33%), sodium hydroxide (NaOH, Labkem, ≥ 97.0%), sodium sulfite (Na_2SO_3, Sigma-Aldrich, 58.5%), *ortho*-phosphoric acid (H_3PO_4, Merck, 85%), and HPLC-grade methanol (CH_3OH, Acros Organics, > 99.99%) were used as received. The following were used as calibration standards: 4-chlorocatechol ($ClC_6H_3(OH)_2$, Sigma-Aldrich, 97%), hydroquinone (Supelco, certified reference material), benzoquinone (Supelco, certified reference material), pyrocatechol (Fluka Chemika, ≥ 99%), maleic acid ($HO_2CCH{=}CHCO_2H$, Acros Organics, ≥ 99%), fumaric acid (HOOCCH=CHCOOH, Fluka Chemika, 99.5%), and formic acid (CH_2O_2, Acros Organics, 99.0%). Deionised water was collected from a Milli-Q water purification unit supplied by Merck.

Analytical techniques. The intermediates produced during the oxidation of 4-chloropehnol were detected using the high-performance liquid chromatography (HPLC) technique. The Waters Alliance 2695 system (WATERS, Milford, CT, USA) equipped with the Waters 2487 Dual λ Absorbance Detector (Waters, Milford, CT, USA) was used for the same. An INERTSIL ODS-3 column (150 mm × 4.6 mm, 5 µm) (GL Sciences, Torrance, CA, USA) was used to detect 4-chlorophenol (CP) and 4-chlorocatechol (4Cl-CC). The methanol:water (30:70, v/v) solvent system buffered with *o*-H_3PO_4 at pH 3 was used as the mobile phase. The flow rate was maintained at 1.0 mL min^{-1} and the sample volume was 1.0 µL. The analytes were detected at 280 nm. Other aromatic compounds such as hydroquinone (HQ), benzoquinone (BQ), and pyrocatechol (CC) were detected under the same conditions. The methanol:water (20:80, v/v) solvent system was used as the mobile phase for eluting the aromatic compounds. The experiments to detect BQ were carried out at a wavelength of 245 nm.

The aliphatic substances (maleic acid, fumaric acid, acetic acid, and formic acid) were separated on the INERTSIL ODS-4 column (250 mm × 4.6 mm, 5 µm) (GL SCIENCES, Torrance, CA, USA). The mobile phase consisted of $(NH_4)_2HPO_4$ (20 mM) at pH 2. The compounds were detected at a wavelength of 214 nm. The flow rate was maintained at 1.0 mL min^{-1}.

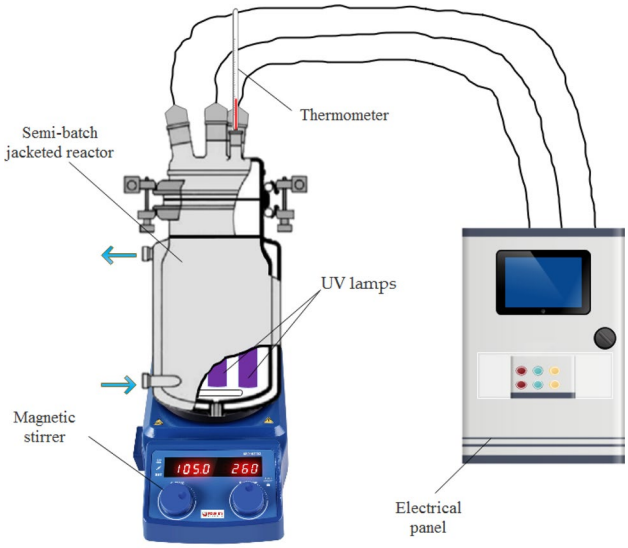

Figure 7. Experimental set-up used to carry out photolytic assays.

The concentration of unreacted H_2O_2 was determined spectrophotometrically at 420 nm, following the procedure outlined by Eisenberg[51]. The variation in the colour intensity was determined by recording the absorbance at 455 nm[52]. The rupture of the aromatic ring was detected by recording the absorbance of the sample at 254 nm using the PerkinElmer Lambda 10 UV/Vis spectrophotometer (Perkinelmer España, Madrid, Spain)[9]. The extent of oxidation was determined as the difference of the initial and final total organic carbon (TOC) using the Shimadzu TOC-VCSN analyser (Izasa Scientific, Alcobendas, Spain) to determine the efficiency of the water treatment process.

The variation in toxicity over time was determined by conducting a MICROTOX toxicity test (ISO 11348-3 (1998); Water Quality—Determination of the inhibitory effect of water samples on the light emission of *Aliivibrio fischeri* (Luminescent bacteria test)—Part 3: Method using freeze-dried bacteria[53]) using a Microtox SDY 500 Analyzer (Microbics Corp., New Castle, DE, USA). The reported method takes into account the changes in the luminescence emission of the luminescent *Aliivibrio fischeri* bacteria when it was exposed to toxic compounds. Toxicity values were expressed in terms of their inhibitory concentration (IC_{50}) or variant effective concentration (EC_{50}) (from the initial concentration of the pollutant (C_i); the dilution necessary to reduce 50% the initial luminescence of the bacteria). These were most commonly expressed in toxicity units (TU) as follows (Eq. 19)[24,26]:

$$Toxicity = \frac{100}{IC_{50}} = \frac{C_i}{EC_{50}}. \tag{19}$$

All samples were treated with excess Na_2SO_3 to remove the residual H_2O_2 present in the system before analysing their toxicities. The samples were aerated to convert the residual sulfite to sulfate[38].

All numerical calculations were performed using the Berkeley Madonna software (version 8.0; UC Berkeley, Berkeley, CA, USA). This software can be used to efficiently solve differential equations to predict the variation in concentrations and toxicities of each group of species over time. In addition, the program used the trial-and-error method to fit experimental and theoretical data to obtain the values of the photolytic, kinetic, and toxicological parameters of grouped substances. The method has been explained in the forthcoming sections.

Experimental set-up. Experiments were performed in a photochemical reactor (2 L batch mode) consisting of a Pyrex mixing vessel. The inner diameter was 100 mm and the height was 270 mm (Fig. 7). The temperature was maintained at 25 ℃ using a jacketed water recirculating thermostatic system. Three low-pressure mercury UV-C lamps (254 nm) that consume a nominal power of 8 W (Philips TUV 8 W G8T5, Philips, Madrid, Spain) were used for irradiation. UV irradiation was used instead of a visible or solar light source because these two sources emit only 5% of the UV irradiation required for the decomposition of hydrogen peroxide. The lamps were equidistant from each other and placed at the centre of the reactor. Each of the lamps was placed inside a quartz tube. Actinometrical measurements, revealed that the incident photonic flux (I_0) was 3.17×10^{-5} Einstein s^{-1}. The effective radiation path (L) was 5.85 cm.

Experimental procedure. 4-chlorophenol was dissolved in water (1.7 L) to obtain a solution of concentration 200 mg L^{-1}. The solution was placed in the reactor and the mixture was stirred using a magnetic stirrer to produce a homogenous solution. Following this, the thermostatic bath was switched on to allow the solution to reach a temperature of 25 ± 1 ℃. The initial ratio of H_2O_2 to 4-chlorophenol (molar ratio (R); UV/H_2O_2 process) ranged from 2 to 400. The initial pH was adjusted as needed. The control sample was collected after adequately

homogenising the solution (homogenisation time: 5 min). Subsequently, the UV-C lamp was switched on and the samples were collected at different time intervals. During the reaction, the temperature of the thermostatic bath was regulated such that the final temperature of the solution was 25 ± 1 °C. All the experiments were conducted thrice. The average standard deviation was less than 5%.

Conclusions

A kinetic model has been proposed to study the changes in the concentration and toxicity during the oxidation process of 4-chlorophenol by UV/H_2O_2. The effect of peroxide dose on degradation was studied to establish the operational conditions that promote the formation of non-toxic or slightly toxic effluents that can be subsequently treated via a biological pathway. The efficiency of the proposed model was calibrated using the experimental data, checking that the mean standard deviation was <0.05.

Based on the identification and analysis of the degradation products, two possible oxidative pathways were proposed, which occur simultaneously. The dose of the oxidant used and the reaction time indicated which of the two pathways would be predominantly operative. The main oxidation intermediates were grouped in different lumps based on various parameters: toxicity, extinction coefficient, and quantum yield.

The model allowed the determination of the kinetic and photolytic parameters. The estimation of these constants allowed the determination of the conditions under which more toxic and recalcitrant by products were formed. Conditions under which less toxic and easily degradable compounds were formed were also determined.

A less toxic effluent (9.95 TU) was produced at a pH of 6.0 when the dose of H_2O_2 was 200 ($R = 200$). Under these conditions, 4-chlorophenol could be degraded completely within 120 min from the start of the reaction. The percentage of mineralisation was approximately 40% and a total loss in colour was observed. This model can be potentially used in industries for the prediction of the operational behaviour of the UV/H_2O_2 system under different working conditions. The model can be used in association with a biological system. Moreover, the behaviour in terms of intermediate formation and toxicity can serve as a reference for other advanced oxidation techniques, including photocatalytic ones, with primary degradation and mineralisation rates similar to those studied here.

Data availability

The datasets generated during and/or analysed during the current study are available from the corresponding author on reasonable request.

Received: 22 March 2021; Accepted: 21 July 2021
Published online: 03 August 2021

References

1. Murcia, M. D. *et al.* Assessing combination treatment, enzymatic oxidation and ultrafiltration in a membrane bioreactor, for 4-chlorophenol removal: Experimental and modeling. *J. Membr. Sci.* **342**, 198–207 (2009).
2. Zhou, T., Li, Y., Ji, J., Wong, F.-S. & Lu, X. Oxidation of 4-chlorophenol in a heterogeneous zero valent iron/H_2O_2 Fenton-like system: Kinetic, pathway and effect factors. *Sep. Purif. Technol.* **62**, 551–558 (2008).
3. Gomez, M. *et al.* A KrCl exciplex flow-through photoreactor for degrading 4-chlorophenol: Experimental and modelling. *Appl. Catal. B* **117–118**, 194–203 (2012).
4. Leyva, E., Crispin, I., Moctezuma, E. & Leyva, S. Selective chemical oxidation or reduction of chlorophenols with potassium nitrosodisulfonate. *ARKIVOC* **2003**, 203–212 (2004).
5. Chung, S.-G. *et al.* Photocatalytic degradation of chlorophenols using star block copolymers: Removal efficiency, by-products and toxicity of catalyst. *Chem. Eng. J.* **215–216**, 921–928 (2013).
6. Valo, R. J., Häggblom, M. M. & Salkinoja-Salonen, M. S. Bioremediation of chlorophenol containing simulated ground water by immobilized bacteria. *Water Res.* **24**, 253–258 (1990).
7. Ettala, M., Koskela, J. & Kiesilä, A. Removal of chlorophenols in a municipal sewage treatment plant using activated sludge. *Water Res.* **26**, 797–804 (1992).
8. Rafiee, M., Mesdaghinia, A., Ghahremani, M. H., Nasseri, S. & Nabizadeh, R. 4-Chlorophenol inhibition on flocculent and granular sludge sequencing batch reactors treating synthetic industrial wastewater. *Desalin. Water Treat.* **49**, 307–316 (2012).
9. Ferreiro, C., Villota, N., Lombraña, J. I. & Rivero, M. J. An efficient catalytic process for the treatment of genotoxic aniline wastewater using a new granular activated carbon-supported titanium dioxide composite. *J. Clean. Prod.* **228**, 1282–1295 (2019).
10. Ferreiro, C., Villota, N., de Luis, A. & Lombrana, J. I. Analysis of the effect of the operational variants in a combined adsorption-ozonation process with granular activated carbon for the treatment of phenol wastewater. *React. Chem. Eng.* **5**, 760–778 (2020).
11. Alfonso-Muniozguren, P. *et al.* Analysis of ultrasonic pre-treatment for the ozonation of humic acids. *Ultrasonics Sonochem.* 105359. https://doi.org/10.1016/j.ultsonch.2020.105359 (2020).
12. Ferreiro, C. *et al.* Analysis of a hybrid suspended-supported photocatalytic reactor for the treatment of wastewater containing benzothiazole and aniline. *Water* **11**, 337 (2019).
13. James, C. P., Germain, E. & Judd, S. Micropollutant removal by advanced oxidation of microfiltered secondary effluent for water reuse. *Sep. Purif. Technol.* **127**, 77–83 (2014).
14. Dixit, A., Tirpude, A. J., Mungray, A. K. & Chakraborty, M. Degradation of 2, 4 DCP by sequential biological-advanced oxidation process using UASB and UV/TiO_2/H_2O_2. *Desalination* **272**, 265–269 (2011).
15. de Luis, A. & Lombraña, J. I. pH-based strategies for an efficient addition of H_2O_2 during ozonation to improve the mineralisation of two contaminants with different degradation resistances. *Water Air Soil Pollut.* **229**, 372 (2018).
16. Marco, A., Esplugas, S. & Saum, G. How and why combine chemical and biological processes for wastewater treatment. *Water Sci. Technol.* **35**, 321–327 (1997).
17. Paul Guin, J., Bhardwaj, Y. K. & Varshney, L. Mineralization and biodegradability enhancement of Methyl Orange dye by an effective advanced oxidation process. *Appl. Radiat. Isotopes* **122**, 153–157 (2017).
18. Çatalkaya, E. Ç., Bali, U. & Şengül, F. Photochemical degradation and mineralization of 4-chlorophenol. *Environ. Sci. Pollut. Res.* **10**, 113–120 (2003).
19. Benitez, F. J., Beltran-Heredia, J., Acero, J. L. & Rubio, F. J. Contribution of free radicals to chlorophenols decomposition by several advanced oxidation processes. *Chemosphere* **41**, 1271–1277 (2000).
20. Ameta, S. *Advanced Oxidation Processes for Wastewater Treatment: Emerging Green Chemical Technology*. (2018).

21. Du, P. *et al.* Transformation, products, and pathways of chlorophenols via electro-enzymatic catalysis: How to control toxic intermediate products. *Chemosphere* **144**, 1674–1681 (2016).
22. Munoz, M., de Pedro, Z. M., Casas, J. A. & Rodriguez, J. J. Assessment of the generation of chlorinated byproducts upon Fenton-like oxidation of chlorophenols at different conditions. *J. Hazard. Mater.* **190**, 993–1000 (2011).
23. Karci, A., Arslan-Alaton, I., Olmez-Hanci, T. & Bekbölet, M. Transformation of 2,4-dichlorophenol by H_2O_2/UV-C, Fenton and photo-Fenton processes: Oxidation products and toxicity evolution. *J. Photochem. Photobiol. A* **230**, 65–73 (2012).
24. Santos, A., Yustos, P., Rodríguez, S., Vicente, F. & Romero, A. Kinetic modeling of toxicity evolution during phenol oxidation. *Ind. Eng. Chem. Res.* **48**, 2844–2850 (2009).
25. Ec, C., U, B. & F, S. Photochemical degradation and mineralization of 4-chlorophenol. *Environ. Sci. Pollut. Res. Int.* 10. https://pubmed.ncbi.nlm.nih.gov/12729044/ (2003).
26. De Luis, A. M., Lombraña, J. I., Menéndez, A. & Sanz, J. Analysis of the toxicity of phenol solutions treated with H_2O_2/UV and H_2O_2/Fe oxidative systems. *Ind. Eng. Chem. Res.* **50**, 1928–1937 (2011).
27. Kumar, A., Sharma, S. K., Sharma, G., Naushad, M. & Stadler, F. J. CeO_2/g-C_3N_4/V_2O_5 ternary nano hetero-structures decorated with CQDs for enhanced photo-reduction capabilities under different light sources: Dual Z-scheme mechanism. *J. Alloys Compds.* **838**, 155692 (2020).
28. Kumar, A. *et al.* High-performance photocatalytic hydrogen production and degradation of levofloxacin by wide spectrum-responsive Ag/Fe_3O_4 bridged $SrTiO_3$/g-C_3N_4 plasmonic nanojunctions: Joint effect of Ag and Fe_3O_4. *ACS Appl. Mater. Interfaces* **10**, 40474–40490 (2018).
29. Kumar, A. *et al.* Bio-inspired and biomaterials-based hybrid photocatalysts for environmental detoxification: A review. *Chem. Eng. J.* **382**, 122937 (2020).
30. Ferreiro, C., Villota, N., Lombraña, J. I. & Rivero, M. J. Heterogeneous catalytic ozonation of aniline-contaminated waters: A three-phase modelling approach using TiO_2/GAC. *Water* **12**, 3448 (2020).
31. Zazo, J. A., Casas, J. A., Mohedano, A. F., Gilarranz, M. A. & Rodríguez, J. J. Chemical pathway and kinetics of phenol oxidation by Fenton's reagent. *Environ. Sci. Technol.* **39**, 9295–9302 (2005).
32. Hirvonen, A., Trapido, M., Hentunen, J. & Tarhanen, J. Formation of hydroxylated and dimeric intermediates during oxidation of chlorinated phenols in aqueous solution. *Chemosphere* **41**, 1211–1218 (2000).
33. Trapido, M., Veressinina, Y., Hentunen, J. K. & Hirvonen, A. Ozonation of chlorophenols: Kinetics, by-products and toxicity. *Environ. Technol.* **18**, 325–332 (1997).
34. Satuf, M. L., Brandi, R. J., Cassano, A. E. & Alfano, O. M. Photocatalytic degradation of 4-chlorophenol: A kinetic study. *Appl. Catal. B* **82**, 37–49 (2008).
35. Murcia, M. D. *et al.* A new substrate and by-product kinetic model for the photodegradation of 4-chlorophenol with KrCl exciplex UV lamp and hydrogen peroxide. *Chem. Eng. J.* **187**, 36–44 (2012).
36. Kusic, H., Koprivanac, N. & Bozic, A. L. Treatment of chlorophenols in water matrix by UV/ferri-oxalate system: Part II. Degradation mechanisms and ecological parameters evaluation. *Desalination* **280**, 208–216 (2011).
37. Hautaniemi, M., Kallas, J., Munter, R. & Trapido, M. Modelling of chlorophenol treatment in aqueous solutions. 1. Ozonation and ozonation combined with UV radiation under acidic conditions. *Ozone Sci. Eng.* **20**, 259–282 (1998).
38. Krebel, M., Kusic, H., Koprivanac, N., Meixner, J. & Bozic, A. L. Treatment of chlorophenols by UV-based processes: Correlation of oxidation by-products, wastewater parameters, and toxicity. *J. Environ. Eng.* **137**, 639–649 (2011).
39. Azevedo, E. B., de Neto, F. R. A. & Dezotti, M. Lumped kinetics and acute toxicity of intermediates in the ozonation of phenol in saline media. *J. Hazard. Mater.* **128**, 182–191 (2006).
40. Kralik, P., Kusic, H., Koprivanac, N. & Loncaric Bozic, A. Degradation of chlorinated hydrocarbons by UV/H_2O_2: The application of experimental design and kinetic modeling approach. *Chem. Eng. J.* **158**, 154–166 (2010).
41. Czaplicka, M. Photo-degradation of chlorophenols in the aqueous solution. *J. Hazard. Mater.* **134**, 45–59 (2006).
42. Mundi, C., Back, M. H. & Back, R. A. Photochemistry of the maleic—Fumaric acid system in aqueous solution at 254 nm. *J. Photochem. Photobiol. A* **67**, 13–22 (1992).
43. Vernon, A. A. & Forbes, G. S. An experiment to determine a photochemical quantum yield. *J. Chem. Educ.* **34**, 350 (1957).
44. Waldner, G., Pourmodjib, M., Bauer, R. & Neumann-Spallart, M. Photoelectrocatalytic degradation of 4-chlorophenol and oxalic acid on titanium dioxide electrodes. *Chemosphere* **50**, 989–998 (2003).
45. Li, X., Cubbage, J. W. & Jenks, W. S. Photocatalytic degradation of 4-chlorophenol. 2. The 4-chlorocatechol pathway. *J. Org. Chem.* **64**, 8525–8536 (1999).
46. Pera-Titus, M., García-Molina, V., Baños, M. A., Giménez, J. & Esplugas, S. Degradation of chlorophenols by means of advanced oxidation processes: A general review. *Appl. Catal. B Environ.* **47**, 219–256 (2004).
47. Bian, W., Song, X., Liu, D., Zhang, J. & Chen, X. The intermediate products in the degradation of 4-chlorophenol by pulsed high voltage discharge in water. *J. Hazard. Mater.* **192**, 1330–1339 (2011).
48. Beltrán, F. J., Rivas, F. J. & Gimeno, O. Comparison between photocatalytic ozonation and other oxidation processes for the removal of phenols from water. *J. Chem. Technol. Biotechnol.* **80**, 973–984 (2005).
49. Rayne, S., Forest, K. & Friesen, K. J. Mechanistic aspects regarding the direct aqueous environmental photochemistry of phenol and its simple halogenated derivatives. A review. *Environ. Int.* **35**, 425–437 (2009).
50. Ronco, A. E., Castillo, G. & DíAz-Baez, M. C. Development and application of microbioassays for routine testing and biomonitoring in Argentina, Chile and Colombia. in *New Microbiotests for Routine Toxicity Screening and Biomonitoring* (eds. Persoone, G., Janssen, C. & De Coen, W.) 49–61. https://doi.org/10.1007/978-1-4615-4289-6_5 (Springer, 2000).
51. Eisenberg, G. Colorimetric determination of hydrogen peroxide. *Ind. Eng. Chem. Anal. Ed.* **15**, 327–328 (1943).
52. Villota, N. *et al.* Colour changes during the carbamazepine oxidation by photo-fenton. *Catalysts* **11**, 386 (2021).
53. Association, A. P. H. *Standard Methods for the Examination of Water & Wastewater*. (American Public Health Association, 2005).

Acknowledgements

The authors are grateful to the University of the Basque Country (UPV/EHU) for their financial support of this study through the PPGA20/33 project, and C. Ferreiro's predoctoral PIF grant (PIF16/367).

Author contributions

J.S. and C.F.: Conceptualisation, Methodology, Investigation, Validation, Data curation, and final editing. N.V.: Write fundamentals and Writing-review. J.I.L. and A.d.L.: Funding acquisition, Resources, and Writing-review. All authors reviewed the manuscript.

Competing interests

The authors declare no competing interests.

Additional information

Supplementary Information The online version contains supplementary material available at https://doi.org/10.1038/s41598-021-95083-7.

Correspondence and requests for materials should be addressed to C.F.

Reprints and permissions information is available at www.nature.com/reprints.

Publisher's note Springer Nature remains neutral with regard to jurisdictional claims in published maps and institutional affiliations.